

RESEARCH ARTICLE

Factorial field manipulation reveals CO₂ and temperature effects on a critical habitat-forming shellfish

Racine E. Rangel^{1,*‡}, Matthew E. S. Bracken¹, Kristy J. Kroeker², Luke P. Miller³ and Cascade J. B. Sorte¹

ABSTRACT

Ocean acidification and warming could have substantial negative impacts on marine organisms, particularly shell-building species. These environmental drivers may operate independently or interactively, amplifying or mitigating their impacts. Previous results have primarily come from lab studies, yet these climate drivers co-occur within naturally dynamic systems with high abiotic and biotic variability. Within intertidal habitats, the impacts of these drivers *in situ* remain poorly understood. We conducted a 6-month field manipulation to determine the effects of ocean acidification and warming on a habitat-forming shellfish, the Pacific blue mussel (*Mytilus trossulus*), in a dynamic intertidal system. Fourteen tide pools containing mussels were manipulated, including ambient (unmanipulated control), CO₂ added, warmed, and combined CO₂ added and warmed treatments. We measured mussel shell thickness, strength and corrosion at 0, 3 and 6 months of exposure to treatment conditions. CO₂ addition led to decreases in shell thickness and strength and increases in shell corrosion. However, we also detected increases in shell strength compared with controls for mussels exposed to both CO₂ addition and warming. These findings indicate that ocean acidification negatively impacted shellfish overall, and the effects of acidification on shell strength might be mitigated under concurrent exposure to moderate warming, leading to an interactive effect of acidification and warming on this critical habitat-forming shellfish.

KEY WORDS: Field experiment, Global change, pH, Rocky intertidal, Shellfish, Temperature

INTRODUCTION

As anthropogenic global change accelerates, there is a pressing need to understand how species will be impacted by concurrent shifts in multiple environmental drivers within natural systems. However, our understanding of species' responses is overwhelmingly informed by studies conducted under laboratory conditions, eliminating the abiotic and biotic variability present in a natural community that could lead to feedback and altered individual- and

population-level responses. In marine systems, increasing greenhouse gas emissions are leading to a decline in seawater pH and carbonate ion concentrations, resulting in ocean acidification (Caldeira and Wickett, 2003; Feely et al., 2009). Acidification can be particularly damaging for species that form calcium carbonate (CaCO₃) exoskeletons or shells, as it causes a reduction in availability of shell-building minerals, such as calcite and aragonite, and can even result in shell dissolution (Feely et al., 2009). Furthermore, ocean acidification is occurring at the same time as ocean temperatures are rising (Cheng et al., 2022), which can influence metabolism and consequently growth and reproduction (Bennett et al., 2019). Thus, acidification and ocean warming pose a risk for ecologically critical and commercially valuable shellfish species (Bullard et al., 2021; Rullens et al., 2019). Yet there is an increasing understanding that seawater pH/carbonate chemistry and temperature can be modified at the local level by abiotic and biotic feedback (Bracken et al., 2018; Ricart et al., 2021; Silbiger and Sorte, 2018; Sorte et al., 2023; Wahl et al., 2018). Here, we took an experimental approach to evaluate the individual and combined impacts of these environmental drivers on a habitat-forming shellfish within the context of a dynamic natural community.

Single climate-driver experiments undertaken in laboratory settings have suggested that ocean acidification and warming are likely to impact shellfish (Beniash et al., 2010; Liu and He, 2012; Ries et al., 2009). For example, acidification has been shown to increase shell corrosion (Melzner et al., 2011; Zhao et al., 2020) and reduce shell thickness (Fitzer et al., 2015a). Weaker and thinner shells are likely to increase vulnerability to fracture and predation (Fitzer et al., 2015a,b). If global change increases the amount of energy required for shell construction and repair, this could result in trade-offs between shell maintenance and other physiological functions such as reproduction (George et al., 2022; Harvey et al., 2016), which may lead to decreased fitness over time (Gaylord et al., 2011). Additionally, projected levels of warming can affect metabolic rates and mortality, as seen in the Mediterranean mussel (*Mytilus galloprovincialis*) (Gazeau et al., 2014). For species already living near their thermal limits, further warming could increase mortality. Although single-climate-driver studies conducted in the laboratory have shown that acidification and warming can independently lead to negative impacts on shellfish, these studies do not account for the fact that in nature, species will be responding to multiple global-change drivers along with other biological and environmental interactions that could alter their responses.

When acidification and warming change in concert, their impacts may affect marine shellfish interactively, amplifying or mitigating single-driver effects (Crain et al., 2008; Kroeker et al., 2014a). In some laboratory studies, the combined effects of acidification and warming have been greater than the responses to single environmental drivers (Byrne and Przeslawski, 2013; Gibson

¹Department of Ecology and Evolutionary Biology, University of California, Irvine, 321 Steinhaus Hall, Irvine, CA 92697, USA. ²Department of Ecology and Evolutionary Biology, University of California, Santa Cruz, Coastal Biology Building, Santa Cruz, CA 95064, USA. ³Department of Biology, San Diego State University, 5500 Campanile Drive, San Diego, CA 92182, USA.

*Present Address: Department of Ecology and Evolutionary Biology, University of California, Santa Cruz, Coastal Biology Building, Santa Cruz, CA 95064, USA.

‡Author for correspondence (raciner@uci.edu)

 R.E.R., 0000-0002-2833-0832

This is an Open Access article distributed under the terms of the Creative Commons Attribution License (<https://creativecommons.org/licenses/by/4.0>), which permits unrestricted use, distribution and reproduction in any medium provided that the original work is properly attributed.

et al., 2011). For example, in the wavy top snail (*Austrocochlea concamerata*), the combined negative impacts of acidification and warming on shell growth and strength were stronger than predicted based on the additive independent effects of these two drivers (Leung et al., 2020). In contrast, the mussel *M. galloprovincialis* grew thicker shells compared with similar controls under moderate warming when it was also exposed to acidification, showcasing a potential mitigating effect (Kroeker et al., 2014a). To best understand how acidification and warming will jointly impact marine shellfish we need to conduct studies under natural conditions in the field.

Natural variation can create unexpected or complex, context-dependent impacts on individuals (Bracken et al., 2018; Kroeker et al., 2016; Ricart et al., 2021; Silbiger and Sorte, 2018) and requires explicit testing with field experiments. In addition to mostly lab-based research (Gunderson et al., 2016) on the effects of acidification and warming, there are a few observational field studies across natural gradients in CO₂ and temperature in unique habitats (Thomsen et al., 2013, 2010; Vargas et al., 2022). Such observational studies have incorporated the variability of dynamic systems that may influence shell traits in calcifying species including changes in temperature, salinity (Sanders et al., 2018), food availability (Melzner et al., 2011; Thomsen et al., 2013), wave exposure (Pfister et al., 2016) or species interactions co-occurring with increased acidification (Kroeker et al., 2014b). However, these are not necessarily perfect analogs to most coastal areas as they rely on unique conditions, such as the presence of high temperature vents and CO₂ vents (Kroeker et al., 2013; Tunnicliffe et al., 2009), or have collinearity between drivers, such as in areas of increased upwelling (Donham et al., 2023). Furthermore, feedback between abiotic and biotic attributes of the ecosystem can lead to results that would be unexpected based on single species or observational studies. In natural systems, there may also be states of refuge from stressful abiotic drivers through local-scale microclimatic variation or periods of temporal recovery (e.g. co-occurrence of species, topographical complexity, diel and seasonal shifts) (Denny et al., 2006; Lima et al., 2016; Ricart et al., 2021; Wahl et al., 2018; Wolfe et al., 2020). For example, in a previous tide pool study, short-term experimental CO₂ addition led to increased (rather than decreased) pH when primary producer abundance was high, possibly because of increased rates of photosynthesis (Bracken et al., 2018). Thus, our understanding of the combined ecological effects of acidification and warming is incomplete because of a lack of studies that incorporate the variability found in natural communities. Ideally, to uncover the emergent effects of continued global change in marine systems, studies would expose ecosystems spanning a range of species composition to randomly determined environmental drivers and measure responses within the context of natural abiotic and biotic feedback.

Here, we used an unprecedented, 6-month-long field manipulation of CO₂ and temperature to ask: how do multiple global-change drivers impact a critical habitat-forming shellfish in an intact and naturally dynamic coastal system? Intertidal marine systems are some of the most environmentally dynamic habitats owing to daily tidal immersion and emersion, and can exhibit fluxes as high as 1.11 pH units and 25.0°C in temperature throughout a single tidal cycle (Denny et al., 2011; Kelly et al., 2011; Wolfe et al., 2020). Tide pools have been utilized as useful test beds to understand physiological responses to changing abiotic conditions, as some species may be living near or at their physiological tolerance limits (Gunderson et al., 2019; Stillman et al., 2025). Thus, research has shown that intertidal diurnal cycles

(i.e. respiration at night and photosynthesis during the day) and resident biota play a regulatory role in temperature and pH conditions within tide pools throughout the tidal cycle (Bracken et al., 2018; Silbiger and Sorte, 2018; Sorte et al., 2023).

The cumulative impacts of multiple climate drivers are increasing, especially within coastal environments (Halpern et al., 2015), and may significantly change shellfish physiology. Shifts in drivers such as pH and temperature are leading to alterations in calcification–dissolution dynamics (Andersson and Gledhill, 2013). Mytilid mussels are habitat-forming calcifying species in coastal habitats worldwide (Seed and Suchanek, 1992). Because adult mussels are sessile, we were able to manipulate and monitor levels of acidification and warming and relate them to shell traits. Shells of *Mytilus trossulus* contain mixed mineralogy (Suzuki and Nagasawa, 2013), including an inner layer of aragonite (nacreous ‘mother of pearl’, which may be more vulnerable to acidification; Doney et al., 2009) and an outer shell layer of calcite (prismatic layer; a more stable calcium carbonate polymorph less prone to dissolution; Kennedy et al., 1969). We quantified the impacts of low tide acidification and daytime warming on shell thickness, strength and corrosion as indicators of shell functionality, stress and, ultimately, vulnerability of this species to mortality (Fitzer et al., 2015b; Telesca et al., 2019; Zhao et al., 2020). We primarily exposed mussels to added CO₂ and warming during low tide [i.e. the most stressful part of the tidal cycle naturally, including the lowest pH, which can lead to increased dissolution particularly at night in the absence of photosynthesis (Kwiatkowski et al., 2016; Silbiger and Sorte, 2018), and the highest temperature, which occurs during daytime low tides (Bracken et al., 2022; Sorte and Bracken, 2015)]. We hypothesized the single driver of warming to have net positive effects, and acidification to have negative impacts, and their combination to have either amplifying (i.e. greater than single drivers alone) or mitigating impacts on shellfish.

MATERIALS AND METHODS

Study location, CO₂ addition and warming experiment, and study organism

Our study site was conducted at John Brown’s Beach on Japonski Island in Sitka, Alaska, USA (57.06°N, 135.37°W), on the ancestral and unceded territory of the Tlingit people. We conducted a factorial manipulation of pH and temperature using 14 of 20 manipulated pools, as six of the pools did not contain mussels naturally (Fig. S1). Tide pools were assigned randomly to four treatments: (1) unmanipulated ($n=3$), (2) CO₂ added ($n=4$), (3) warmed ($n=4$) and (4) CO₂ added+warmed ($n=3$). The pools containing mussels were located between the mid and high intertidal zone at an average tide height (all values are means±1 s.d.) of 2.60±0.36 m above mean lower-low water with volumes of 13.18±8.20 liters and a volume range from 3.0 to 28.0 liters (Table 1).

Tide pools were exposed to CO₂ and warming manipulations over a 6-month period from April to September 2019 primarily during low tide (~66% of time), when the pools were isolated from the ocean. Tide pool pH levels were manipulated using yeast reactors, as in Sorte and Bracken (2015). A waterproof box was anchored next to the pool and filled with 500 ml warm tap water, 60 g sugar, 0.7 g baker’s yeast and 2 g NaHCO₃ to buffer the internal pH of the reactor. From the yeast reactor housing unit, CO₂ flowed into an airline tube connected to an air stone anchored within the pool (Fig. S2). Solutions within the reactors were replaced every 3 days to maintain reduced pH conditions in CO₂ added pools. Temperature was manipulated using a microcontroller and two rechargeable 14 A-h gel cell batteries that were housed within a

Table 1. Tide pool characteristics, treatments and mean±s.d. mussel percent cover and wet biomass per treatment over the 6-month CO₂ + warming manipulations at three time points of exposure (0=pre-manipulation, and after 3 and 6 months) when *Mytilus trossulus* were collected from pools for shell analyses

Pool number	Treatment	Volume (l)	Tide height (m)	Mussel percent cover (%)			Normalized mussel biomass (g l ⁻¹)		
				0	3	6	0	3	6
7	U	28.0	2.63	14.2±8.2	19.0±11.5	19.4±10.5	111.4±109.3	150.2±129.5	114.2±75.6
10	U	5.5	2.30						
31	U	6.5	2.86						
9	C	3.0	2.23	29.7±24.1	22.8±18.5	14.6±13.7	452.1±717.9	344.2±546.0	310.8±476.5
15	C	5.0	2.30						
27	C	12.5	2.87						
35	C	9.0	3.09						
8	W	7.0	2.65	9.0±6.6	10.7±8.8	11.5±7.2	41.7±56.1	41.4±48.8	66.9±49.7
13	W	22.0	2.36						
16	W	19.5	1.99						
33	W	25.0	2.94						
5	C+W	8.0	2.46	16.1±9.5	18.5±11.7	14.5±11.1	74.2±48.2	100.4±117.6	131.3±128.5
11	C+W	14.0	2.48						
36	C+W	19.5	3.23						

U, unmanipulated; C, CO₂ added; W, warmed; C+W, CO₂ added+warmed. The 14 tide pools contained mussels during the experimental time period and were used in this study. Note that the pools are part of a fully factorially manipulated design ($N=20$ pools); further details on all 20 pools can be found in Bracken et al. (2022) and Sorte et al. (2023).

separate waterproof box anchored next to the pools (Fig. S2). The batteries were connected to submerged heating elements anchored within the tide pool. The warming treatments were only active during daytime low tides (Miller and Long, 2015) and simulated warmer daytime tides. Batteries within the waterproof boxes were switched out and functioning of heaters and yeast reactors was confirmed daily.

We quantified impacts of pH and temperature on the Pacific blue mussel (*Mytilus trossulus* Gould 1850), which was the most common sessile invertebrate at our site (Fig. S1). One mussel per experimental pool was haphazardly collected from submerged mussel clumps at three time points (0, 3 and 6 months; Table 1). Across pools, we collected individual mussels over a span of 2 to 4 days at each time point. Mussel sample size decreased throughout the experiment as all mussels in some of the treatment pools died during manipulations (tide pools 35 and 36 after July). Mussels collected were of similar size (all values mean±s.d.) with standard length=22.62±1.94 mm, depth (height)=8.21±0.84 mm, shell width=11.14±0.94 mm and dried shell mass=1.33±0.32 g. To track changes in *M. trossulus* abundance throughout the CO₂ and warming manipulations, we conducted intertidal community surveys at each sampling time point (Fig. S1) as in Sorte and Bracken (2015). The community changes associated with these manipulations are the focus of additional studies.

Tide pool data collection

To determine the influence of our manipulations on water parameters of the tide pools, we conducted discrete water monitoring and sampling during one daytime and one nighttime low tide at each of the sampling time points (six total monitoring events): day and night at time 0 (prior to the manipulations in late March), after 3 months (July) and after 6 months (September). During each sampling event, we measured water temperature, salinity and dissolved oxygen with a ProDSS optical DO meter (YSI, Inc., Yellow Springs, OH, USA), and pH (mV) with an HI9829 Meter 7609829 glass pH electrode (Hanna Instruments, Woonsocket, RI, USA) at three sampling points during the daytime or nighttime low tide. Sampling took place while the tide pools were separated from the ocean approximately 2.75±0.04 h (mean±s.d.) after tidal emersion. At the same time as water parameters were measured with handheld instruments, we

collected 250 ml of seawater for total alkalinity (TA) analysis. Dark glass bottles were spiked with 60 µl of mercuric chloride, and TA (µmol kg⁻¹) was determined via auto-titration (Metrohm Titrando 905, Herisau, Switzerland). Salinity, water temperature, TA and calculated total scale pH collected during the last sampling point (longest time separated from the ocean) for 0, 3 and 6 months were used to determine saturation states of aragonite (Ω_{Ar}) and calcite (Ω_{Ca}), and the calculation of P_{CO_2} and dissolved inorganic carbon (DIC) values using the *seacarb* package in R. All shell analyses used the values from the last water samples collected as indicators of pH levels within the tide pools.

Continuous tide pool temperatures were measured within each of the tide pools using HOBO TidbiT loggers (Onset, Bourne, MA, USA; ±0.2°C accuracy) that recorded temperature every 5 min through the duration of the manipulations. Based on known shore heights of each pool and observed tide data from Sitka Harbor, Baranof Island, Sitka, Alaska (tbone tides; <https://tide.arthroinfo.org/>), all temperature data were sorted to contain only low daytime and nighttime tide values. Neither daily average nor daily 99th percentile of tide pool temperatures differed between treatments prior to manipulations (at time 0; $P>0.218$; Table S1). For further analyses, we used daily 99th percentile maximum temperatures as they are likely an indicator of thermal stress to the mussels within the tide pools.

Shell thickness, strength and corrosion analyses

To determine the impacts of acidification, warming and their combined effects on *M. trossulus* shells, we quantified shell thickness, strength and corrosion. The number of mussel shells used in each analysis varied owing to the nature of each measurement (e.g. cracks in shells rendered individual shells unsuitable for strength analysis), and the number (n) of shells used for each measurement is listed in Table 2. Shell thickness was measured at three locations on the shell – base (1 mm from the anterior edge of the shell), middle and lip (1 mm from the posterior edge of the shell) – using micrometer calipers (Fowler High Precision, Canton, MA, USA). Each measurement was standardized by dividing by total shell length (Sherker et al., 2017).

We measured shell strength using an Instron® universal testing system (Instron®, Norwood, MA, USA). Strength was assessed for

Table 2. The number of shells tested (*n*) for each shell measurement at all three time points of exposure (0=pre-manipulation, and after 3 and 6 months) for unmanipulated and all CO₂ + warming treatments

	Shell thickness			Shell strength			Shell corrosion					
							Inner			Outer		
Time of exposure	0	3	6	0	3	6	0	3	6	0	3	6
Unmanipulated	3	3	3	3	3	3	3	3	3	3	3	3
CO ₂ added	4	4	3	4	4	2	4	4	3	4	4	3
Warmed	4	4	3	4	4	3	4	4	3	4	4	3
CO ₂ added+warmed	3	3	2	3	4	2	3	3	2	3	3	2

The *n* of shells can vary due to each shell measurement having different standards for testing; see Materials and Methods for further details. Shell thickness measurements were made at the lip, middle and base for all individuals.

the right valve of each mussel; left valves were used if the right valve was fractured or cracked, and no strength sample was collected if visible cracks were seen in both valves. Valves were placed between the horizontal plates of the testing machine (Fig. S3) and were compressed at a constant loading rate of 1 mm min⁻¹. The continuous force was recorded by a computer until failure of the shell, and the force (N) required to break the shell (maximum compression load) was recorded (Barclay et al., 2019; Zhao et al., 2020). Each strength measurement was standardized by dividing by the total shell length.

Shell corrosion changes were assessed by quantifying the corrosion of the inner and outer surface of the right valves; again, left valves were used if the right valve was completely fractured and no valves were assessed if both valves were completely fractured. Each valve was placed under a Leica EZ 4W stereomicroscope (Leica Microsystems, Wetzlar, Germany) and 3–14 images were taken at 10X magnification to obtain high resolution photographs to identify corrosion. Autostitch software (Brown and Lowe, 2007) was used to merge the photos to create a composite image of each whole valve (Fig. S4). Using image analysis software (ImageJ 1.8.0_172), with the scale set at 100 pixels=1.0 mm, the mussel valve and corroded area were traced to determine total and corroded surface area, respectively. After loss of the periostracum, corroded regions of the shell lose the typical glossy and reflective appearance. We were able to visually identify shell corrosion under a light source and assess visual corrosion not due to breakage and chipping (Melnzer et al., 2011; Fig. S4). Percent corrosion was calculated by dividing the corroded area by the shell area and multiplying by 100.

Statistical analyses

We used generalized linear models (GLMs) to evaluate the effects of treatments and their interaction on pH levels, temperatures and the shell metrics thickness, strength and corrosion at 0, 3 and 6 months of exposure. To avoid issues of overfitting and non-independence across repeated samplings within tide pools, analyses for each time point (0, 3 and 6 months) were run separately and the simplest model was maintained, and we used treatments as categorical factors in all models. Final models accounted for the factorial design by including time of day, CO₂ treatment (ambient or CO₂ added), temperature treatment (ambient or warmed) and their interaction (CO₂ treatment×temperature treatment). For analyses of strength and thickness, a Gaussian distribution was used (Shapiro–Wilk test for normality, *P*>0.05) and outer shell corrosion data were square root transformed to meet the normality assumption. For analyses of inner shell corrosion, a gamma distribution was used after adding half of the smallest corrosion rate from our dataset as a percentage (1.57%) to each 0 value to meet requirements of the analysis (Barclay et al., 2019; Berry, 1987). Additionally, pH (time 3), temperature (time points 0, 3 and 6 months) and thickness (time 6) were positively

skewed, so gamma distributions were used. Models were run and residuals were checked and confirmed using the *performance* package (Lüdecke et al., 2021), after which we calculated summary analyses of deviance tables with *F*-tests to determine the significance of factors and interaction terms. The *emmeans* package (<https://CRAN.R-project.org/package=emmeans>) was used for Tukey *post hoc* tests of differences between treatments. All statistical analyses were carried out in R v.4.2.2 (<https://www.r-project.org/>). All means are presented ±s.d.

RESULTS

Impacts of temperature and pH environmental treatments on this habitat-forming shellfish emerged after 3 to 6 months of exposure within a natural community. Despite natural variability inherent in the tide pools, there were no differences for any of the shell metrics between treatments prior to the manipulations at time 0 (*P*≥0.092; Tables 3–6). Additionally, there were only moderate changes in mussel abundance throughout the experiment; further details on community-level responses to these manipulations can be found in Rangel (2023) and Sorte, C. J. B., Miller, L. P., Rangel, R. E., Kroeker, K. J. and Bracken, M. E. (unpublished data). However, the addition of CO₂ to the tide pools strongly impacted shell functionality, including thickness, strength and corrosion. Furthermore, the impacts of the CO₂ addition treatment were modified by warming, particularly the emergent effects on shell strength and corrosion. These alterations occurred despite high variability in the tide pool characteristics, a relatively high level of acidification and a moderate effect of warming on the pools.

Throughout all the time points (0, 3 and 6 months), tide pool pH varied between daytime and nighttime values (all *P*≤0.0002; Tables S1, S2; Fig. 1). Tide pool pH was lower in tide pools with CO₂ addition during the 0, 3 and 6 month surveys, although only significantly so at 3 months (*F*_{1,26}=34.48, *P*<0.001; Fig. 1A; Tables S1, S2). Additionally, prior to the start of the manipulations (time 0), the CO₂ addition pools tended to have lower pH values during the daytime samplings than the CO₂ added+warmed treatments (CO₂ added=8.68, CO₂ added+warmed=9.09), and this was observed at time point 3 (6.90, 7.53) and time point 6 (7.54, 7.69) (Table 3), although these pools were not significantly differently in pH across any of the time points (*P*≥0.474; Table S1). Prior to the start of manipulations (time 0), *P*_{CO₂} of the pools on average ranged from 8.35 to 156 μatm during daytime tides and 621 to 866 μatm during nighttime tides (Table 3). After the manipulations were started (i.e. at 3 and 6 months), the *P*_{CO₂} of the pools on average ranged from 64.36 to 10,241 μatm during daytime tides and 2306 to 11,110 μatm during nighttime tides. Additionally, DIC prior to the start of manipulations (time 0) on average ranged from 735 to 1177 μmol kg⁻¹ during daytime tides and 1703 to 1835 μmol kg⁻¹ during nighttime tides (Table 3). After the manipulations were started (3 and 6 months), the DIC of the

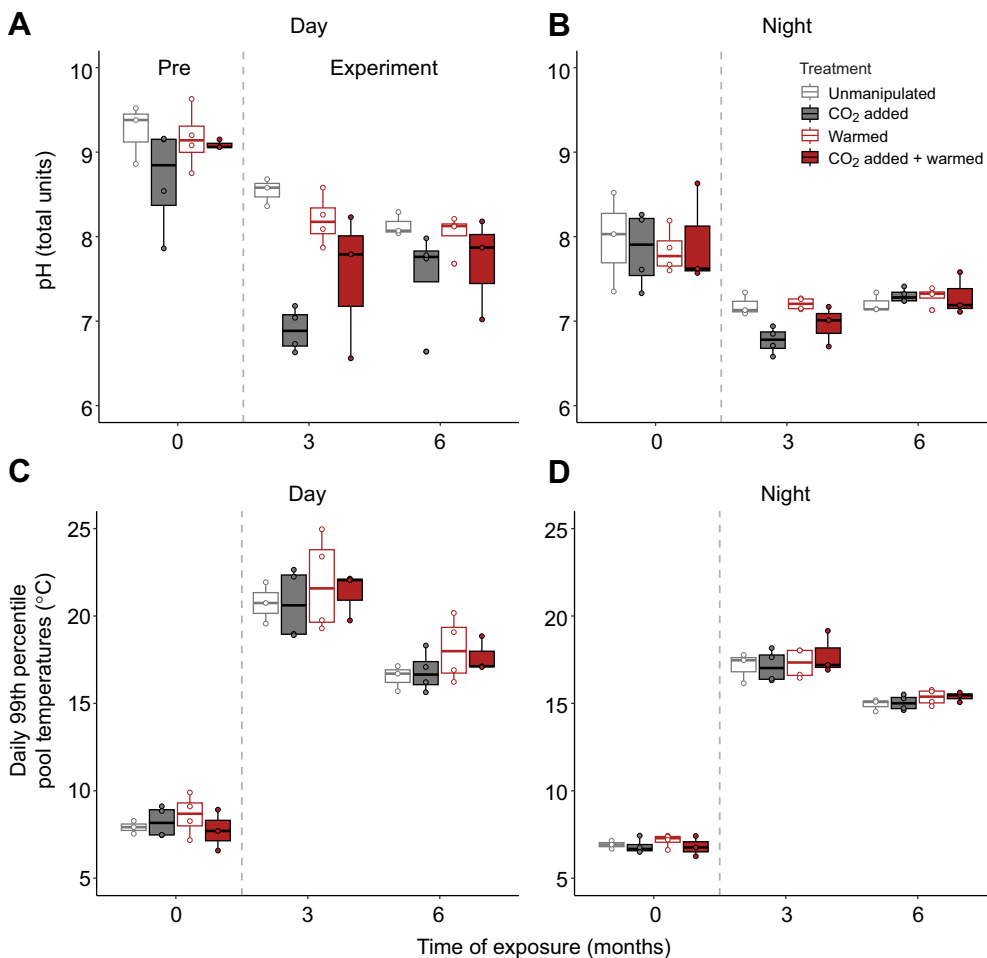


Fig. 1. Tide pool pH and temperature across the experimental time points. (A,C) Daytime and (B,D) nighttime (A,B) pH and (C,D) mean daily 99th percentile temperatures from tide pools after 0 (pre-manipulation) and after the experiment started at 3, and 6 months of exposure to CO₂ and warming manipulations. Measurements were made during low tides during discrete water sampling events (for pH) or recorded every 5 min for $N=28$ days (prior to each sampling event) with submerged data loggers (for temperature). Treatments include unmanipulated (open gray), CO₂ added (gray solid), warmed (open red), and CO₂ added+warmed (red solid). Warmed treatments were shut off during nighttime tides. Dashed lines represent the start of the CO₂ and warming manipulations. Boxplots show data within the 25th to the 75th percentiles, with the middle solid line representing the median, and whiskers showing highest and lowest values within 1.5-fold of this range. Data points indicate individual tide pools. Values are for 14 pools that contain mussels with unmanipulated ($n=3$), CO₂ added ($n=4$), warmed ($n=4$) and CO₂ added+warmed ($n=3$) tide pools.

pools on average ranged from 1134 to 2903 $\mu\text{mol kg}^{-1}$ during daytime tides and 1919 to 2935 $\mu\text{mol kg}^{-1}$ during nighttime tides. On average, CO₂ addition reduced pH in the tide pools by 0.49 ± 0.05 total pH units.

Overall, during daytime low tides during manipulations, there was an average increase in the 99th percentile of pool temperatures in warmed versus unwarmed tide pools of $1.1 \pm 0.16^\circ\text{C}$. When accounting for both low daytime and nighttime tides, the average between warmed versus unwarmed pools was $0.7 \pm 0.31^\circ\text{C}$. These results indicate that although the warming treatment tended to increase the frequency of high temperature periods during daytime tides when the heaters were on, there was high variability between pools (Fig. S5), and these differences were not statistically significant after *post hoc* comparisons across the 14 pools used in this study ($P \geq 0.359$; Table S2).

Across the shell thickness measurements located at the lip, middle point and base of the mussel shell (Fig. 2, Table 4), the CO₂ addition treatment reduced shell thickness at the middle point (Fig. 2B) after 3 months ($F_{1,12}=8.75$, $P=0.014$) and 6 months of exposure ($F_{1,9}=6.42$, $P=0.039$). After 6 months, the CO₂ addition treatment also decreased thickness at the shell base ($F_{1,9}=5.60$, $P=0.050$; Fig. 2C), whereas in the warming treatment thickness increased at the base ($F_{1,8}=9.69$, $P=0.017$). *Post hoc* comparisons indicated that the base of shells from mussels in CO₂ addition pools were thinner than from those in the warmed pools ($t=3.843$, $P=0.026$; Table S3). Shell lip thickness increased in the CO₂ added+warmed pools after 3 months ($F_{1,10}=6.46$, $P=0.029$) and within the CO₂ added pools after 6 months ($F_{1,9}=6.19$, $P=0.042$).

Shell strength decreased under the elevated CO₂ treatment except when concurrently exposed to warmed conditions (CO₂ added+warmed treatment), where shell strength actually increased (Fig. 3, Table 5). Shell strength was not influenced by CO₂ addition or warming after 3 months of exposure ($P \geq 0.187$). However, after 6 months of exposure, warming ($F_{1,7}=8.04$, $P=0.030$) and the combined effects of CO₂ addition and warming ($F_{1,6}=19.91$, $P=0.004$) impacted shell strength. *Post hoc* comparisons revealed that adding CO₂ led to weaker shells when compared with shells of mussels living under ambient levels of CO₂ ($t=-3.404$, $P=0.054$; Table S4), and CO₂ added+warmed shells were 120% stronger than CO₂ added shells ($t=5.250$, $P=0.008$; Table S4). Shells of mussels that experienced both CO₂ addition and warming were 47% stronger than those exposed to warming alone, and 36% stronger than mussels living under ambient (unmanipulated) conditions, although these were not significantly different in *post hoc* comparisons ($P \geq 0.189$, Table S4).

CO₂ addition also drove increases in mussel shell corrosion (Fig. 4). There were no effects of the CO₂ addition treatment or the warming treatment on shell corrosion after 3 months of exposure ($P \geq 0.180$; Table 6). However, after 6 months of exposure, CO₂ addition led to increased corrosion on the outer shell ($F_{1,9}=5.91$, $P=0.045$) when compared with natural corrosion levels in unmanipulated pools ($t=-3.250$, $P=0.054$; Table S5). Similarly, CO₂ addition increased inner shell corrosion after 6 months of exposure ($F_{1,9}=10.57$, $P=0.014$), as did exposure to CO₂ addition and warming together ($F_{1,7}=5.70$, $P=0.048$) compared with controls ($t=4.425$, $P=0.013$; Table S5). The negative impact of CO₂ addition

Table 3. Environmental conditions across tide pool CO₂ + warming manipulation treatments during discrete water sampling events (N=14 pools)

Time point	Treatment	n	Temperature (°C)		pH (total units)		DO (mg l ⁻¹)		Salinity (ppt)		TA (μmol kg ⁻¹)		Ω _{Ar}		Ω _{Ca}		P _{CO₂} in situ (μatm)		DIC (μmol kg ⁻¹)	
			Day	Night	Day	Night	Day	Night	Day	Night	Day	Night	Day	Night	Day	Night	Day	Night	Day	Night
0	U	3	11.63±0.85	6.83±0.29	9.25±0.35	7.97±0.59	18.94±0.06	5.25±2.78	31.7±0.36	30.9±0.69	1408±35	1851±40	5.53±1.02	1.62±1.51	8.73±1.60	2.59±2.42	8.35±11.05	743±933	735±187	1720±197
	C	4	11.05±1.42	7.47±0.82	8.68±0.62	7.85±0.45	13.96±0.38	5.59±2.42	32.2±0.76	31.2±0.57	1603±237	1925±81	4.02±2.37	1.25±0.94	6.34±3.71	1.98±1.49	156±257	866±885	1177±486	1837±198
	W	4	11.88±2.19	7.50±0.36	9.16±0.36	7.83±0.26	18.4±2.31	4.41±0.64	32.3±1.31	30.7±0.66	1486±265	1823±119	5.42±1.15	0.98±0.61	8.53±1.80	1.56±0.97	13.69±18.83	621±316	831±352	1750±107
3	C+W	3	10.90±2.35	7.10±0.46	9.09±0.05	7.94±0.60	18.2±2.42	5.79±4.41	32.0±0.63	30.8±0.45	1622±20	1845±108	6.14±0.04	1.71±2.08	9.69±0.10	2.72±3.32	10.30±1.69	667±522	948±33	1703±128
	U	3	18.23±0.40	15.50±0.17	8.54±0.16	7.19±0.13	15.93±0.69	2.68±0.48	30.6±0.06	30.2±0.45	1536±220	2100±42	3.86±1.39	0.34±0.11	6.02±2.17	0.54±0.17	64.39±24.36	3277±969	1134±97	2190±74
	C	4	18.15±0.81	15.75±0.44	8.90±0.26	6.77±0.16	13.97±0.72	3.07±0.84	31.0±1.16	30.7±0.36	2619±346	2540±481	0.29±0.21	0.16±0.04	0.45±0.33	0.25±0.07	8853±4787	11,110±6252	2903±342	2935±694
6	W	4	17.90±0.70	15.53±0.15	8.20±0.30	7.20±0.07	12.4±4.73	2.85±0.75	30.5±0.26	30.3±0.55	1799±116	2144±89	2.69±1.21	0.36±0.05	4.21±1.89	0.56±0.07	265±196	3145±624	1539±221	2228±114
	C+W	3	18.20±0.36	15.67±0.64	7.53±0.87	6.96±0.24	13.14±0.92	3.16±0.47	31.7±1.82	30.7±0.86	2661±1650	2577±667	1.25±1.05	0.25±0.07	0.95±1.65	0.39±0.11	10.241±17.025	8079±6714	2881±2324	2846±921
	C	3	13.93±0.15	12.43±0.25	8.13±0.14	7.21±0.12	10.5±0.41	2.48±0.26	21.5±8.34	17.3±8.69	1558±441	1863±463	1.56±0.90	0.21±0.14	2.52±1.40	0.35±0.22	247±86.32	3003±871	1419±368	1976±462
C	U	4	13.95±0.10	12.38±0.25	7.54±0.61	7.30±0.08	11.1±2.96	3.07±0.85	20.7±3.54	20.2±6.33	1996±409	1843±204	0.71±0.45	0.26±0.07	1.16±0.72	0.43±0.11	4330±7392	2306±552	2115±760	1919±217
	W	4	13.93±0.10	12.62±0.48	8.04±0.24	7.29±0.11	9.88±3.64	2.05±0.98	25.4±1.41	22.7±5.31	1836±150	2034±66	1.60±0.59	0.31±0.07	2.57±0.93	0.50±0.11	431±355	2545±650	1701±202	2115±61
	C+W	3	14.00±0.17	12.57±0.15	7.69±0.60	7.29±0.25	10.8±2.36	3.14±2.63	27.1±2.12	26.5±1.78	1990±14	2072±58	1.25±1.05	0.37±0.20	1.98±1.67	0.59±0.33	1805±2414	2728±1348	1945±201	2152±133

Means±s.d. values for environmental conditions at the different time points of exposure (0, pre-manipulation, and after 3 and 6 months) by treatment for the last sampling point during each low tide series. U, unmanipulated; C, CO₂ addition; W, warmed; C+W, CO₂ added + warmed [from tide pools where mussels (*M. trossulus*) were collected]. Temperature, pH, dissolved oxygen (DO) and salinity were measured with handheld instruments while total alkalinity (TA) values were measured via titration of discrete water samples and used to calculate the *in situ* saturation states of aragonite and calcite (Ω_{Ar}, Ω_{Ca}). DIC and P_{CO₂} were calculated using the seacarb package in R (Brackeen et al., 2018) and we note that the error propagation for the DIC calculated from pH and TA is 8.9 ±0.67 mmol kg⁻¹ for daytime and 7.7±0.50 mmol kg⁻¹ for nighttime values.

on shell corrosion was slightly diminished when acidification was experienced concurrent with warmer conditions (Fig. 4), although the CO₂ added+warmed treatments did not differ from the CO₂ added shells ($r=-0.261$, $P=0.993$; Table S5).

DISCUSSION

Based on the results of our field manipulations of CO₂ and temperature, we demonstrated that acidification and warming impact shell integrity and function of a common and important shellfish within 3 months, and that interactive, emergent effects of multiple drivers are exhibited within 6 months. Specifically, acidification led to shells that were thinner, weaker and more corroded. However, when CO₂ additions were combined with warming, these effects were diminished for both shell strength and corrosion, which may be due to warming lessening the effects of the CO₂ treatments. Impacts of CO₂ addition and warming on shell thickness were detected after 3 months and impacts on shell strength and corrosion were detected after 6 months of exposure. These results suggest that *in situ* exposure to acidification can greatly impact the construction and function of calcifying structures in shellfish. Furthermore, despite the relatively moderate changes in temperature in our study, the effects of CO₂ addition on the mussels were offset, highlighting the potential mitigating effects of moderate warming on the impacts of acidification.

Acidification led to the shell becoming thinner at the midpoint, and weaker overall, as well as more corroded on both the outside and inside of the shells. These results are similar to those measured in the lab, where shellfish species exhibit more corroded, brittle, thinner and weaker shells owing to reductions of shell growth, repair and biomineralization under increased CO₂ stress (Fitzer et al., 2015b; Lee et al., 2021; Li et al., 2015). Our results highlight these same trends within a natural community; however, we are unable to identify an exact mechanism. Thus, it is likely that under increased acidification, *M. trossulus* individuals reallocated energy resources across physiological processes and, specifically, between shell growth and repair among the three regions of the shell. We found that the lip, and to some degree, the base, of the shells was thicker when exposed to acidification at the end of the 6-month manipulation, although these changes were not significantly different from the unmanipulated pools. Dynamic coastal systems exhibit variation in environmental parameters such as temperature, pH, salinity and DIC as well as variation in predator presence (e.g. sea stars, crabs and whelks) that may influence shell characteristics (Fitzer et al., 2018; Legrand et al., 2018; Sanders et al., 2018; Sherker et al., 2017; Wolfe et al., 2020). Thus, the variation in shell thickness pre-manipulation and subsequent increases in the lip and base thickness over time may be a response to seasonal shifts in environmental conditions. *Mytilus* species increase shell growth and byssal thread attachment strength in response to higher wave energy (Babarro and Carrington, 2013) and strong coastal storms (Carrington, 2002), which are common in the autumn, winter and spring months along the Alaskan coastline (Bromirski et al., 2017; Mock and Dodds, 2009). However, whether due to shifts in energy resources or reductions in repair, despite some increases in lip and base shell thickness, decreased middle shell thickness in concert with increased inner shell corrosion over time resulted in weaker shells. Thus, although mussel shell growth (i.e. generally measured by length from base to lip) may appear to continue to increase as normal under future acidic conditions (Byrne and Fitzer, 2019), our study shows that acidification leads to middle sections of the shell thinning, causing the shell to become more fragile.

Whereas the acidification treatment alone had negative effects on shell structure, the combined treatment of CO₂ addition and

Table 4. Results from analyses of deviance tables by the *F*-test method for the generalized linear models to determine the effect of CO₂ added, warmed and CO₂ added + warmed at time point 0 (pre-manipulations), and after 3 and 6 months of exposure to climate change manipulations on the standardized shell thickness of the mussel *M. trossulus* at the lip, middle and base of the shell

	Time point	Factor	d.f.	Residual d.f.	F-value	P-value
Lip	0	CO ₂ added	1	12	0.614	0.451
		Warmed	1	11	1.641	0.229
		CO ₂ added+warmed	1	10	3.030	0.112
	3	CO ₂ added	1	12	0.296	0.598
		Warmed	1	11	0.321	0.583
		CO ₂ added+warmed	1	10	6.462	0.029
	6	CO ₂ added	1	9	6.192	0.042
		Warmed	1	8	0.022	0.887
		CO ₂ added+warmed	1	7	0.443	0.527
	0	CO ₂ added	1	12	0.014	0.907
		Warmed	1	11	1.404	0.264
		CO ₂ added+warmed	1	10	1.694	0.222
Middle	3	CO ₂ added	1	12	8.754	0.014
		Warmed	1	11	0.093	0.766
		CO ₂ added+warmed	1	10	0.746	0.408
	6	CO ₂ added	1	9	6.423	0.039
		Warmed	1	8	0.273	0.618
		CO ₂ added+warmed	1	7	1.355	0.283
	0	CO ₂ added	1	12	0.965	0.349
		Warmed	1	11	0.337	0.574
		CO ₂ added+warmed	1	10	1.404	0.264
	3	CO ₂ added	1	12	0.450	0.517
		Warmed	1	11	0.297	0.598
		CO ₂ added+warmed	1	10	0.283	0.607
Base	6	CO ₂ added	1	9	5.599	0.050
		Warmed	1	8	9.689	0.017
		CO ₂ added+warmed	1	7	0.000	1.000

Significant *P*-values are in bold.

warming resulted in an antagonistic effect, causing shells to be stronger and less corroded relative to shells of *M. trossulus* from tide pools receiving CO₂ addition alone. This could be due to natural variability unrelated to the treatments (e.g. variability in temperature and total alkalinity among pools associated with freshwater input). For example, aragonite is the stronger of the two calcium carbonate polymorphs (Lowenstam, 1954), and within our pools, the CO₂ added+warmed pools tended to have higher saturation states of aragonite compared with the CO₂ added pools, but not compared with the unmanipulated pools. Although we did not directly measure impacts on layering of the mussel shells within this study, calcifying shellfish can alter shell strength by adjusting the layering and packing of various calcium carbonate polymorphs (Leung et al., 2020). Future research identifying alterations in shell layering mechanisms and into inner shell degradation in response to climate drivers detectable through microscopy (Fitzer et al., 2019) would be beneficial. Thus, increased shell strength in the combined CO₂ added+warmed pools may be because the saturation states of aragonite and calcite were higher in the CO₂ added+warmed pools, leading to easier precipitation of these shell-building compounds for added layering and increased strength (Mucci, 1983).

However, note that for some mussel species, physiology and food availability play a larger role than saturation states in mediating shell repair and growth (Kroeker et al., 2014a; Mackenzie et al., 2014).

Mytilus trossulus can exhibit decreased feeding rates coupled with higher growth rates after acclimation to fluctuating temperatures within laboratory settings, which may be due to changes in assimilation efficiency, cost of tissue maintenance or controlled food availability (Marshall et al., 2021). Thus, the type or availability of food may play a role in mediating shell traits in the field. In our study, increased stressful conditions at low tide may have caused mussels to close their shells (Clarke and Griffiths, 1990) and enter an anaerobic state, limiting feeding, and potentially resulting in reductions in shell repair and increased impacts on shell traits. We did not directly track food availability for the mussels within the tide pools; however, during our experiment, the mean±s.d. monthly satellite chlorophyll concentrations were 0.9±0.4 µg l⁻¹ within the Sitka Channel. For similar *Mytilus* species, individuals will continue to filter feed even at lower concentrations of chlorophyll between 0.5 and 0.9 µg l⁻¹ (Larsen et al., 2018). Based on these values, *M. trossulus* may be food limited based on phytoplankton availability at our site. However, we also note that *M. trossulus* populations (e.g. in the northern Gulf of Alaska) can be heavily dependent on macroalgal detritus and rely less on phytoplankton (Corliss et al., 2024), which may mitigate limited food availability. Mussels can also take up carbon directly from the environment or use internal carbon stores via a temperature-dependent metabolic pathway for shell building (Lee et al., 2021;

Table 5. Results from analyses of deviance tables by the *F*-test method for the generalized linear models to determine the effect of CO₂ added, warmed and CO₂ added + warmed at time point 0 (pre-manipulations), and after 3 and 6 months of exposure to climate change manipulations on the standardized shell strength of the mussel *M. trossulus*

Time point	Factor	d.f.	Residual d.f.	F-value	P-value
0	CO ₂ added	1	12	0.015	0.907
	Warmed	1	11	1.192	0.301
	CO ₂ added+warmed	1	10	2.971	0.116
3	CO ₂ added	1	12	2.003	0.187
	Warmed	1	11	0.859	0.376
	CO ₂ added+warmed	1	10	1.055	0.329
6	CO ₂ added	1	8	0.124	0.737
	Warmed	1	7	8.038	0.030
	CO ₂ added+warmed	1	6	19.913	0.004

Significant *P*-values are in bold.

Table 6. Results from analyses of deviance tables by the *F*-test method for the generalized linear models to determine the effect of CO₂ added, warmed and CO₂ added + warmed at time point 0 (pre-manipulations), and after 3 and 6 months of exposure to climate change manipulations on the outer and inner shell corrosion of the mussel *M. trossulus*

	Time point	Factor	d.f.	Residual d.f.	<i>F</i> -value	<i>P</i> -value
Outer shell	0	CO ₂ added	1	12	0.050	0.828
		Warmed	1	11	1.428	0.260
		CO ₂ added+warmed	1	10	0.898	0.366
	3	CO ₂ added	1	12	2.078	0.180
		Warmed	1	11	0.061	0.456
		CO ₂ added+warmed	1	10	1.865	0.202
	6	CO ₂ added	1	9	5.913	0.045
		Warmed	1	8	0.108	0.752
		CO ₂ added+warmed	1	7	4.547	0.070
Inner shell	0	CO ₂ added	1	12	3.484	0.092
		Warmed	1	11	0.029	0.869
		CO ₂ added+warmed	1	10	0.073	0.792
	3	CO ₂ added	1	12	2.200	0.169
		Warmed	1	11	2.257	0.164
		CO ₂ added+warmed	1	10	0.169	0.690
	6	CO ₂ added	1	9	10.571	0.014
		Warmed	1	8	4.511	0.071
		CO ₂ added+warmed	1	7	5.701	0.048

Significant *P*-values are in bold.

Romanek et al., 1992). Based on lab studies, under acidified conditions, the metabolic carbon uptake pathway may be less energetically costly compared with using an environmental carbon source (Lee et al., 2021; Lu et al., 2018). For example, in a laboratory study, *M. edulis* held under acidified and warmed conditions decreased their use of environmental carbon sources at the lowest pH of 7.7 from ~66% to 62%, although this shift was not significantly different between temperatures (Lu et al., 2018). However, this shift in use of metabolic carbon is unlikely to be sustained for long periods of time (Lee et al., 2021). Importantly, these individuals were held at constant pH and temperature environments in the lab for 5 weeks and fed every 2 days. Our

study allowed individuals to feed naturally in the tide pools, including the presence of macroalgae within and adjacent to our experimental site that could allow for a more consistent pathway for food uptake and for continued growth and shell maintenance. This field experiment was also maintained for a longer period of time (i.e. 6 months) and allowed for natural variation in pH and temperature change throughout tidal cycles. Thus, in laboratory studies it may be harder to determine the mitigating impacts of moderate warming as we demonstrate here in a natural system.

That we found marked, mitigating impacts of the warming treatment was particularly interesting given the relative magnitude of changes in pH and temperature in our experiment. We

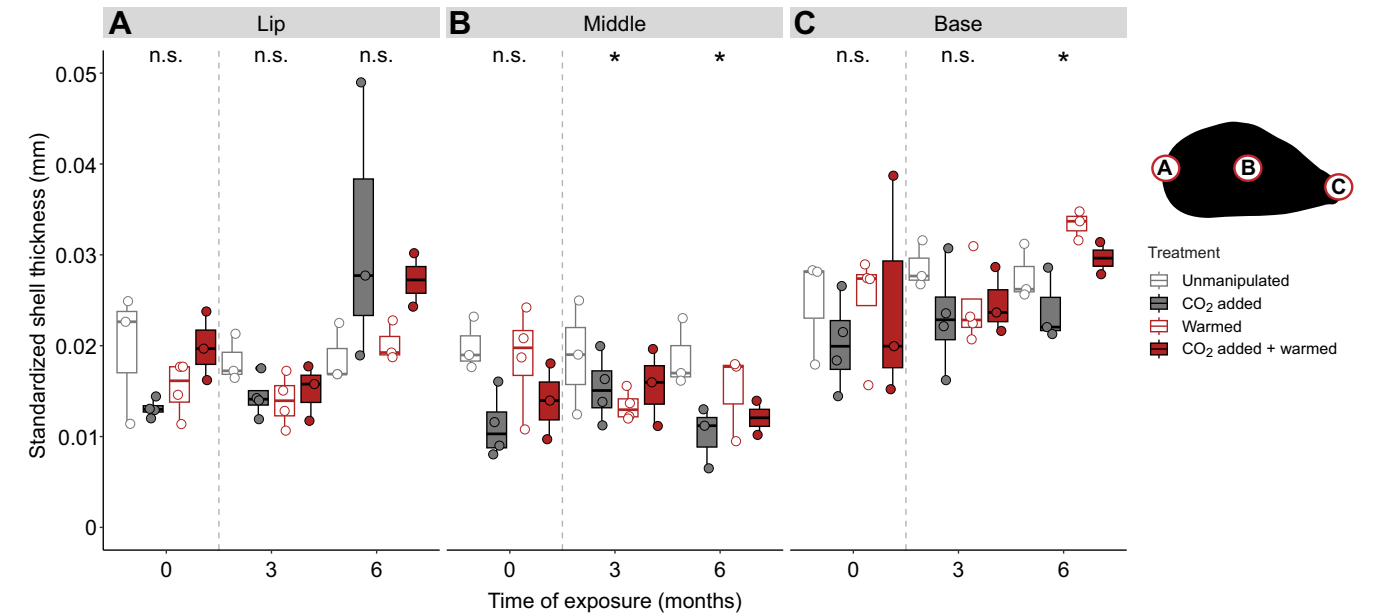


Fig. 2. Standardized shell thickness across time of exposure to CO₂ and warming manipulations based on measurements at three locations on the mussel shells. (A) Lip, (B) middle point and (C) base. Boxplots show data within the 25th to the 75th percentiles, with the middle solid line representing the median, and whiskers showing highest and lowest values within 1.5-fold of this range. Data points indicate individual mussels from tide pools. The treatments at 0, 3 and 6 months of exposure and shell location (lip, middle and base) include unmanipulated (*n*=3/3/3), CO₂ added (*n*=4/4/3), warmed (*n*=4/4/3) and CO₂ added+warmed (*n*=3/3/2) tide pools. See Table 2 for further details on sample size. Dashed line indicates when manipulations were started and treatment colors and shading are as in Fig. 1; separate time point analyses using GLM models and Tukey *post hoc* tests indicate whether treatments are significant (**P*<0.05; n.s., *P*>0.05), with further details on statistical analysis detailed in the Materials and Methods.

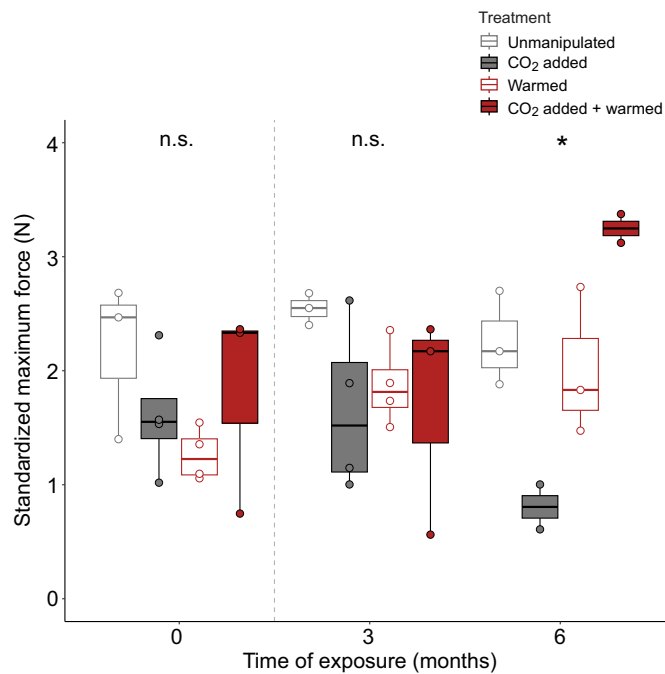


Fig. 3. Mussel shell strength as indicated by the maximum force necessary to break the shells across the time of exposure to CO₂ and warming manipulation treatments. Boxplots show data within the 25th to the 75th percentiles, with the middle solid line representing the median, and whiskers showing highest and lowest values within 1.5-fold of this range. Data points indicate individual mussels from tide pools at 0, 3 and 6 months of exposure. The treatments include unmanipulated ($n=3/3/3$), CO₂ added ($n=4/4/2$), warmed ($n=4/4/3$) and CO₂ added+warmed ($n=3/4/2$) tide pools. See Table 2 for further details on sample size. Dashed line indicates when manipulations were started and treatment colors and shading are as in Fig. 1; separate time point analyses using GLM models and Tukey *post hoc* tests indicate whether treatments are significant (* $P<0.05$; n.s., $P>0.05$).

experimentally manipulated acidity by reducing pH, on average by 0.49 ± 0.05 pH units. Although climate models predict that surface water of the global ocean will decrease by 0.1–0.4 pH units by year 2100 (Garcia-Soto et al., 2021; Masson-Delmotte et al., 2021), the changes in local tide pools may vary from the global ocean. We projected changes in DIC associated with a change from current 400 to future 800 μatm to our calculated DIC measurements (added 200 $\mu\text{mol l}^{-1}$ of DIC) in our tide pools. The projected DIC measurements for daytime range from 1748 to 5239 $\mu\text{mol kg}^{-1}$, and for nighttime from 1627 to 3598 $\mu\text{mol kg}^{-1}$, and the projected pH changes were calculated to be 0.36 ± 0.25 pH units during the daytime and 0.24 ± 0.13 pH units during the nighttime. In contrast, increases in tide pool temperature were relatively modest (by $1.1\pm0.16^\circ\text{C}$), as climate models predict a further increase in sea surface temperatures of $0.54\text{--}2.5^\circ\text{C}$ by 2100 (Masson-Delmotte et al., 2021; Ruela et al., 2020). This modest effect of warming may be due to only operating the heaters during daytime tides. Given the relative magnitude of changes in pH and temperature, as well as our focus on shell traits, it is perhaps not surprising that we found stronger impacts of acidification than warming, when applied separately. However, despite these exposure levels, we found emergent effects of both acidification and warming when combined.

The ecological impacts of acidification and warming on individuals can scale up to influence community composition and ecosystem-level processes (Barry et al., 1995; Harley, 2011). Despite the limitations to our study (including low replication and

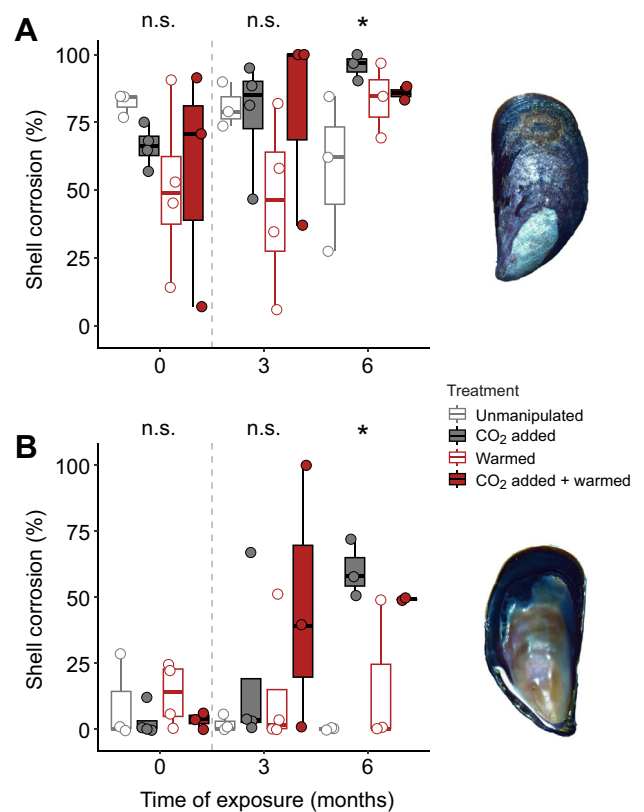


Fig. 4. Percent corrosion for the mussel shells across time of exposure to CO₂ and warming manipulations. (A) Outer shell and (B) inner shell. Boxplots show data within the 25th to the 75th percentiles, with the middle solid line representing the median, and whiskers showing highest and lowest values within 1.5-fold of this range. Data points indicate individual mussels from tide pools at 0, 3 and 6 months of exposure for the inner and outer portion of the shell. The treatments include unmanipulated ($n=3/3/3$, $3/3/3$), CO₂ added ($n=4/4/3$, $4/4/3$), warmed ($n=4/4/3$, $4/4/3$) and CO₂ added+warmed ($n=3/3/2$, $3/3/2$) tide pools. See Table 2 for further details on sample size. Dashed line indicates when manipulations were started and treatment colors and shading are as in Fig. 1; separate time point analyses using GLM models and Tukey *post hoc* tests indicate whether treatments are significant (* $P<0.05$; n.s., $P>0.05$).

environmental conditions that could not be manipulated such as nighttime temperature and total alkalinity), we discovered emergent alterations in shell thickness, corrosion and strength after exposure to acidification and warming. Our study encompassed a wide range of natural variation, increasing the likelihood that alterations in shell traits are a result of our manipulations and not underlying natural variation, with potentially important implications for ecological function. Shell strength is a key functional trait that helps to defend shellfish against predation and changes in environmental drivers (Crane et al., 2021). At our field site, the majority of potential predators include birds and dogwhelks, as well as lower densities of other predatory snails and crabs, which feed on shellfish, including mussels, by drilling or crushing through the exterior shell (Rovero et al., 1999; Telesca et al., 2021). During our study, the average densities of the dogwhelk *Nucella lima* (a drilling predator) ranged from 5.4 individuals m^{-2} in March to 14.1 individuals m^{-2} in July within the experimental pools. The main crab species besides *Pagurus* spp. was the purple shore crab (*Hemigrapsus nudus*), which primarily feed on algae and small snails, as well as oyster seed (Lord, 2017; Yamada and Boulding, 1998); thus, they may also feed on smaller mussels or newly settled recruits. Thinner, weaker

and more corroded shells may lead to increased consumption of *M. trossulus* by these predators (Lowen et al., 2013; Sherker et al., 2017), resulting in changes in *M. trossulus* population densities and the functions they provide to the community and ecosystem. Beyond the increased vulnerability inherent in reduced shell functionality, increasing CO₂ and warming could have direct, lethal effects. During our field study, we observed mass mortality and an overall decrease of all sessile species in two tide pools (pools 35 and 36, a CO₂ added pool and a CO₂ added+warmed pool, respectively) between 3 and 6 months of exposure. These pools were the highest on the shore of all 14 pools included in our study with mussels in them. Additionally, the dominant red macroalgae (*Neorhodomela* spp.) cause relatively modest effects on pH changes within coastal systems (Mahanes et al., 2023; Tharaldson, 2018). Therefore, the mussels in our study may have had decreased resilience to the natural variability of pH and temperature with little to no mitigating effect even with the co-occurrence of abundant, photosynthesizing macroalgae. This result suggests that amelioration of acidification and warming may be a viable mechanism depending on the species present, and until physiological limits are surpassed. Any mass mortality of *M. trossulus* would result in loss of critical habitat for numerous benthic organisms, directly driving changes in biodiversity, food webs, biogeochemistry, shoreline stabilization and water quality regulation in this and other coastal communities (Fields and Silbiger, 2022; Gazeau et al., 2013; Rullens et al., 2019).

Our study suggests that acidification together with warming affects shell structure and function in a critical, habitat-forming shellfish within a natural system. Acidification led to decreases in shell integrity and function, while moderate warming mitigated the negative impacts of acidification on some shell traits including strength and corrosion. That there is high natural variability in both pH and temperature in tide pools suggests that intertidal species are acclimated and adapted to a broad range of pH and temperature conditions (Kwiatkowski et al., 2016; Legrand et al., 2018; Rangel and Sorte, 2022; Wolfe et al., 2020). However, even relatively small departures from this natural variability can lead to significant harm, as seen in the alterations in sublethal shell traits we measured as well as observed instances of mass mortality. Overall, the results from this study highlight the importance of conducting experiments in natural systems, and not just under controlled laboratory conditions, to better predict how multiple global change drivers impact ecologically valuable shellfish species.

Acknowledgements

We are thankful to all members of the Sitka NSF team, who aided in the execution of the field surveys, experiment, and data management: G. Bernatchez, E. O'Brien, S. Mastroni, L. Strobe, L. Pandori, K. Monuki, L. Bell, J. Gomez, M. Schouweiler, G. Houghton, S. Garcia, Z. Danielson, U. Hoshijima, G. Gallaher, J. C. Basile and J. Viramontes. We thank A. Vara and V. Lau for assistance with mussel shell thickness and corrosion measurements; B. Gaylord, A. Saley and A. Smart for assistance and access to the Instron universal testing system; N. Silbiger for assistance with data analysis; and R. Macias for microscope access and assistance in photographing the mussel shells. We thank D. German and past and present Sorte lab members who provided helpful feedback on this research at various stages. We are also thankful for partnerships with the Sitka Sound Science Center, US Coast Guard Air Station Sitka and the University of Alaska, Southeast.

Competing interests

The authors declare no competing or financial interests.

Author contributions

Conceptualization: R.E.R., C.J.B.S.; Data curation: R.E.R.; Formal analysis: R.E.R.; Funding acquisition: R.E.R., M.E.S.B., K.J.K., L.P.M., C.J.B.S.; Investigation: R.E.R., M.E.S.B., L.P.M., C.J.B.S.; Methodology: R.E.R., M.E.S.B., K.J.K., L.P.M., C.J.B.S.; Project administration: R.E.R.; Resources: R.E.R., M.E.S.B., K.J.K., L.P.M., C.J.B.S.;

Software: R.E.R.; Validation: R.E.R.; Visualization: R.E.R.; Supervision: R.E.R., M.E.S.B., C.J.B.S.; Project administration: R.E.R.; Writing – original draft: R.E.R.; Writing – review & editing: R.E.R., M.E.S.B., K.J.K., L.P.M., C.J.B.S.

Funding

This research was supported by the National Science Foundation (OCE-1756173 to C.J.B.S. and M.E.S.B., OCE-1904185 to L.P.M. and OCE-1756208 to K.J.K.), the Society for Integrative & Comparative Biology Grant-in-Aid of Research, and American Microscopical Society Student Research Grant to R.E.R. R.E.R. was also supported by the National Academy of Sciences, Engineering, and Medicine on behalf of the Ford Foundation. Open Access funding provided by University of California. Deposited in PMC for immediate release.

Data and resource availability

All of the data and code that support the findings of this study are publicly available in the Dryad Digital Repository at <https://doi.org/10.7280/D1P10V> (Rangel et al., 2025) and within the Github repository titled 'Sitka-Mussel-Shell' at <https://github.com/racine-rangel/Sitka-Mussel-Shell>.

ECR Spotlight

This article has an associated ECR Spotlight interview with Racine Rangel.

References

- Andersson, A. J. and Gledhill, D. (2013). Ocean acidification and coral reefs: effects on breakdown, dissolution, and net ecosystem calcification. *Annu. Rev. Mar. Sci.* **5**, 321–348. doi:10.1146/annurev-marine-121211-172241
- Babarro, J. M. and Carrington, E. (2013). Attachment strength of the mussel *Mytilus galloprovincialis*: effect of habitat and body size. *J. Exp. Mar. Biol. Ecol.* **443**, 188–196. doi:10.1016/j.jembe.2013.02.035
- Barclay, K. M., Gaylord, B., Jellison, B. M., Shukla, P., Sanford, E. and Leighton, L. R. (2019). Variation in the effects of ocean acidification on shell growth and strength in two intertidal gastropods. *Mar. Ecol. Prog. Ser.* **626**, 109–121. doi:10.3354/meps13056
- Barry, J. P., Baxter, C. H., Sagarin, R. D. and Gilman, S. E. (1995). Climate-related, long-term faunal changes in a California rocky intertidal community. *Science* **267**, 672–675. doi:10.1126/science.267.5198.672
- Beniash, E., Ivanina, A., Lieb, N. S., Kurochkin, I. and Sokolova, I. M. (2010). Elevated level of carbon dioxide affects metabolism and shell formation in oysters *Crassostrea virginica*. *Mar. Ecol. Prog. Ser.* **419**, 95–108. doi:10.3354/meps08841
- Bennett, S., Duarte, C. M., Marbà, N. and Wernberg, T. (2019). Integrating within-species variation in thermal physiology into climate change ecology. *Philos. Trans. R. Soc. B* **374**, 20180550. doi:10.1098/rstb.2018.0550
- Berry, D. A. (1987). Logarithmic transformations in ANOVA. *Biometrics* **43**, 439–456. doi:10.2307/2531826
- Bracken, M. E. S., Silbiger, N. J., Bernatchez, G. and Sorte, C. J. B. (2018). Primary producers may ameliorate impacts of daytime CO₂ addition in a coastal marine ecosystem. *PeerJ* **6**, e4739. doi:10.7717/peerj.4739
- Bracken, M. E. S., Miller, L. P., Mastroni, S. E., Lira, S. M. and Sorte, C. J. B. (2022). Accounting for variation in temperature and oxygen availability when quantifying marine ecosystem metabolism. *Sci. Rep.* **12**, 825. doi:10.1038/s41598-021-04685-8
- Bromirski, P. D., Flick, R. E. and Miller, A. J. (2017). Storm surge along the Pacific coast of North America. *J. Geophys. Res. Oceans* **122**, 441–457. doi:10.1002/2016JC012178
- Brown, M. and Lowe, D. G. (2007). Automatic panoramic image stitching using invariant features. *Int. J. Comput. Vis.* **74**, 59–73. doi:10.1007/s11263-006-0002-3
- Bullard, E. M., Torres, I., Ren, T., Graeve, O. A. and Roy, K. (2021). Shell mineralogy of a foundational marine species, *Mytilus californianus*, over half a century in a changing ocean. *Proc. Natl. Acad. Sci. USA* **118**, e2004769118. doi:10.1073/pnas.2004769118
- Byrne, M. and Fitzer, S. (2019). The impact of environmental acidification on the microstructure and mechanical integrity of marine invertebrate skeletons. *Conserv. Physiol.* **7**, coz062. doi:10.1093/conphys/coz062
- Byrne, M. and Przeslawski, R. (2013). Multistressor impacts of warming and acidification of the ocean on marine invertebrates' life histories. *Integr. Comp. Biol.* **53**, 582–596. doi:10.1093/icb/ict049
- Caldeira, K. and Wickett, M. E. (2003). Anthropogenic carbon and ocean pH. *Nature* **425**, 365. doi:10.1038/425365a
- Carrington, E. (2002). Seasonal variation in the attachment strength of blue mussels: causes and consequences. *Limnol. Oceanogr.* **47**, 1723–1733. doi:10.4319/lo.2002.47.6.1723
- Cheng, L., von Schuckmann, K., Abraham, J. P., Trenberth, K. E., Mann, M. E., Zanna, L., England, M. H., Zika, J. D., Fasullo, J. T., Yu, Y. et al. (2022). Past and future ocean warming. *Nat. Rev. Earth Environ.* **3**, 1–19. doi:10.1038/s43017-022-00345-1
- Clarke, B. and Griffiths, C. (1990). Ecological energetics of mussels *Choromytilus meridionalis* under simulated intertidal rock pool conditions. *J. Exp. Mar. Biol. Ecol.* **137**, 63–77. doi:10.1016/0022-0981(90)90060-P

- Corliss, K., von Biela, V., Coletti, H., Bodkin, J., Esler, D. and Iken, K. (2024). Relative importance of macroalgae and phytoplankton to nearshore consumers and growth across climatic conditions in the northern Gulf of Alaska. *Estuaries Coast.* **47**, 1579–1597. doi:10.1007/s12237-024-01371-6
- Crain, C. M., Kroeker, K. and Halpern, B. S. (2008). Interactive and cumulative effects of multiple human stressors in marine systems. *Ecol. Lett.* **11**, 1304–1315. doi:10.1111/j.1461-0248.2008.01253.x
- Crane, R., Diaz Reyes, J. and Denny, M. (2021). Bivalves rapidly repair shells damaged by fatigue and bolster strength. *J. Exp. Biol.* **224**, jeb242681. doi:10.1242/jeb.242681
- Denny, M. W., Miller, L. P. and Harley, C. D. (2006). Thermal stress on intertidal limpets: long-term hindcasts and lethal limits. *J. Exp. Biol.* **209**, 2420–2431. doi:10.1242/jeb.02258
- Denny, M. W., Dowd, W. W., Bilir, L. and Mach, K. J. (2011). Spreading the risk: small-scale body temperature variation among intertidal organisms and its implications for species persistence. *J. Exp. Mar. Biol. Ecol.* **400**, 175–190. doi:10.1016/j.jembe.2011.02.006
- Doney, S. C., Balch, W. M., Fabry, V. J. and Feely, R. A. (2009). Ocean acidification: a critical emerging problem for the ocean sciences. *Oceanography* **22**, 16–25. doi:10.5670/oceanog.2009.93
- Donham, E. M., Flores, I., Hooper, A., O'Brien, E., Vylet, K., Takeshita, Y., Freiwald, J. and Kroeker, K. J. (2023). Population-specific vulnerability to ocean change in a multistressor environment. *Sci. Adv.* **9**, eade2365. doi:10.1126/sciadv.ade2365
- Feely, R. A., Doney, S. C. and Cooley, S. R. (2009). Ocean acidification: present conditions and future changes in a high-CO₂ world. *Oceanography* **22**, 36–47. doi:10.5670/oceanog.2009.95
- Fields, J. and Silbiger, N. (2022). Foundation species loss alters multiple ecosystem functions within temperate tidepool communities. *Mar. Ecol. Prog. Ser.* **683**, 1–19. doi:10.3354/meps13978
- Fitzer, S. C., Vittert, L., Bowman, A., Kamenos, N. A., Phoenix, V. R. and Cusack, M. (2015a). Ocean acidification and temperature increase impact mussel shell shape and thickness: problematic for protection? *Ecol. Evol.* **5**, 4875–4884. doi:10.1002/ecs3.1756
- Fitzer, S. C., Zhu, W., Tanner, K. E., Phoenix, V. R., Kamenos, N. A. and Cusack, M. (2015b). Ocean acidification alters the material properties of *Mytilus edulis* shells. *J. R. Soc. Interface* **12**, 20141227. doi:10.1098/rsif.2014.1227
- Fitzer, S. C., Torres Gabarda, S., Daly, L., Hughes, B., Dove, M., O'Connor, W., Potts, J., Scanes, P. and Byrne, M. (2018). Coastal acidification impacts on shell mineral structure of bivalve mollusks. *Ecol. Evol.* **8**, 8973–8984. doi:10.1002/ecs3.4416
- Fitzer, S. C., Bin San Chan, V., Meng, Y., Chandra Rajan, K., Suzuki, M., Not, C., Toyofuku, T. and Fal, L. (2019). Established and emerging techniques for characterising the formation, structure and performance of calcified structures under ocean acidification. *Oceanogr. Mar. Biol. Annu. Rev.* **57**, 89–126.
- Garcia-Soto, C., Cheng, L., Caesar, L., Schmidtko, S., Jewett, E. B., Cheripka, A., Rigor, I., Caballero, A., Chiba, S., Báez, J. C. et al. (2021). An overview of ocean climate change indicators: sea surface temperature, ocean heat content, ocean pH, dissolved oxygen concentration, Arctic Sea ice extent, thickness and volume, sea level and strength of the AMOC (Atlantic Meridional Overturning Circulation). *Front. Mar. Sci.* **8**, 642372. doi:10.3389/fmars.2021.642372
- Gaylord, B., Hill, T. M., Sanford, E., Lenz, E. A., Jacobs, L. A., Sato, K. N., Russell, A. D. and Hettinger, A. (2011). Functional impacts of ocean acidification in an ecologically critical foundation species. *J. Exp. Biol.* **214**, 2586–2594. doi:10.1242/jeb.055939
- Gazeau, F., Parker, L. M., Comeau, S., Gattuso, J.-P., O'Connor, W. A., Martin, S., Pörtner, H.-O. and Ross, P. M. (2013). Impacts of ocean acidification on marine shelled molluscs. *Mar. Biol.* **160**, 2207–2245. doi:10.1007/s00227-013-2219-3
- Gazeau, F., Alliouane, S., Bock, C., Bramanti, L., López Correa, M., Gentile, M., Hirse, T., Pörtner, H.-O. and Ziveri, P. (2014). Impact of ocean acidification and warming on the Mediterranean mussel (*Mytilus galloprovincialis*). *Front. Mar. Sci.* **1**, 62. doi:10.3389/fmars.2014.00062
- George, M. N., O'Donnell, M. J., Concodello, M. and Carrington, E. (2022). Mussels repair shell damage despite limitations imposed by ocean acidification. *J. Mar. Sci. Eng.* **10**, 359. doi:10.3390/jmse10030359
- Gibson, R., Atkinson, R., Gordon, J., Smith, I. and Hughes, D. (2011). Impact of ocean warming and ocean acidification on marine invertebrate life history stages: vulnerabilities and potential for persistence in a changing ocean. *Oceanogr. Mar. Biol. Annu. Rev.* **49**, 1–42.
- Gunderson, A. R., Armstrong, E. J. and Stillman, J. H. (2016). Multiple stressors in a changing world: the need for an improved perspective on physiological responses to the dynamic marine environment. *Annu. Rev. Mar. Sci.* **8**, 357–378. doi:10.1146/annurev-marine-122414-033953
- Gunderson, A. R., Abegaz, M., Ceja, A. Y., Lam, E., Souther, B. F., Boyer, K., King, E., You Mak, K. T., Tsukimura, B. and Stillman, J. H. (2019). Hot rocks and not-so-hot rocks on the seashore: patterns and body-size dependent consequences of microclimatic variation in intertidal zone boulder habitat. *Integr. Org. Biol.* **1**, obz024. doi:10.1093/iob/obz024
- Halpern, B. S., Frazier, M., Potapenko, J., Casey, K. S., Koenig, K., Longo, C., Lowndes, J. S., Rockwood, R. C., Selig, E. R., Selkoe, K. A. et al. (2015). Spatial and temporal changes in cumulative human impacts on the world's ocean. *Nat. Commun.* **6**, 7615. doi:10.1038/ncomms8615
- Harley, C. D. (2011). Climate change, keystone predation, and biodiversity loss. *Science* **334**, 1124–1127. doi:10.1126/science.1210199
- Harvey, B. P., McKeown, N. J., Rastrick, S. P., Bertolini, C., Foggo, A., Graham, H., Hall-Spencer, J. M., Milazzo, M., Shaw, P. W., Small, D. P. et al. (2016). Individual and population-level responses to ocean acidification. *Sci. Rep.* **6**, 1–7. doi:10.1038/srep20194
- Kelly, M. W., Sanford, E. and Grosberg, R. K. (2011). Limited potential for adaptation to climate change in a broadly distributed marine crustacean. *Proc. R. Soc. B* **279**, 349–356. doi:10.1098/rspb.2011.0542
- Kennedy, W. J., Taylor, J. D. and Hall, A. (1969). Environmental and biological controls on bivalve shell mineralogy. *Biol. Rev.* **44**, 499–530. doi:10.1111/j.1469-185X.1969.tb00610.x
- Kroeker, K. J., Gambi, M. C. and Micheli, F. (2013). Community dynamics and ecosystem simplification in a high-CO₂ ocean. *Proc. Natl Acad. Sci. USA* **110**, 12721–12726. doi:10.1073/pnas.1216464110
- Kroeker, K. J., Gaylord, B., Hill, T. M., Hosfelt, J. D., Miller, S. H. and Sanford, E. (2014a). The role of temperature in determining species' vulnerability to ocean acidification: a case study using *Mytilus galloprovincialis*. *PLoS ONE* **9**, e100353. doi:10.1371/journal.pone.0100353
- Kroeker, K. J., Sanford, E., Jellison, B. M. and Gaylord, B. (2014b). Predicting the effects of ocean acidification on predator–prey interactions: a conceptual framework based on coastal molluscs. *Biol. Bull.* **226**, 211–222. doi:10.1086/BBLv226n3p211
- Kroeker, K. J., Sanford, E., Rose, J. M., Blanchette, C. A., Chan, F., Chavez, F. P., Gaylord, B., Helmuth, B., Hill, T. M., Hofmann, G. E. et al. (2016). Interacting environmental mosaics drive geographic variation in mussel performance and predation vulnerability. *Ecol. Lett.* **19**, 771–779. doi:10.1111/ele.12613
- Kwiatkowski, L., Gaylord, B., Hill, T., Hosfelt, J., Kroeker, K. J., Nebuchina, Y., Ninokawa, A., Russell, A. D., Rivest, E. B., Sesboué, M. et al. (2016). Nighttime dissolution in a temperate coastal ocean ecosystem increases under acidification. *Sci. Rep.* **6**, 1–9. doi:10.1038/srep22984
- Larsen, P. S., Luskow, F. and Riisgård, H. U. (2018). Too much food may cause reduced growth of blue mussels (*Mytilus edulis*) – test of hypothesis and new 'high Chl a BEG-model'. *J. Mar. Syst.* **180**, 299–306. doi:10.1016/j.jmarsys.2018.01.011
- Lee, T. H., McGill, R. A. and Fitzer, S. (2021). Effects of extra feeding combined with ocean acidification and increased temperature on the carbon isotope values ($\delta^{13}\text{C}$) in the mussel shell. *J. Exp. Mar. Biol. Ecol.* **541**, 151562. doi:10.1016/j.jembe.2021.151562
- Legrand, E., Riera, P., Pouliquen, L., Bohner, O., Cariou, T. and Martin, S. (2018). Ecological characterization of intertidal rockpools: seasonal and diurnal monitoring of physico-chemical parameters. *Reg. Stud. Mar. Sci.* **17**, 1–10. doi:10.1016/j.rsmas.2017.11.003
- Leung, J. Y., Russell, B. D. and Connell, S. D. (2020). Linking energy budget to physiological adaptation: how a calcifying gastropod adjusts or succumbs to ocean acidification and warming. *Sci. Total Environ.* **715**, 136939. doi:10.1016/j.scitotenv.2020.136939
- Li, S., Liu, C., Huang, J., Liu, Y., Zheng, G., Xie, L. and Zhang, R. (2015). Interactive effects of seawater acidification and elevated temperature on biomineralization and amino acid metabolism in the mussel *Mytilus edulis*. *J. Exp. Biol.* **218**, 3623–3631.
- Lima, F. P., Gomes, F., Seabra, R., Wetthey, D. S., Seabra, M. I., Cruz, T., Santos, A. M. and Hilbish, T. J. (2016). Loss of thermal refugia near equatorial range limits. *Glob. Change Biol.* **22**, 254–263. doi:10.1111/gcb.13115
- Liu, W. and He, M. (2012). Effects of ocean acidification on the metabolic rates of three species of bivalve from southern coast of China. *Chin. J. Oceanol. Limnol.* **30**, 206–211. doi:10.1007/s00343-012-1067-1
- Lord, J. P. (2017). Potential impact of the Asian shore crab *Hemigrapsus sanguineus* on native northeast Pacific crabs. *Biol. Invasions* **19**, 1879–1887. doi:10.1007/s10530-017-1399-z
- Lowen, J., Innes, D. and Thompson, R. (2013). Predator-induced defenses differ between sympatric *Mytilus edulis* and *M. trossulus*. *Mar. Ecol. Prog. Ser.* **475**, 135–143. doi:10.3354/meps10106
- Lowenstam, H. A. (1954). Factors affecting the aragonite: calcite ratios in carbonate-secreting marine organisms. *J. Geol.* **62**, 284–322. doi:10.1086/626163
- Lu, Y., Wang, L., Wang, L., Cong, Y., Yang, G. and Zhao, L. (2018). Deciphering carbon sources of mussel shell carbonate under experimental ocean acidification and warming. *Mar. Environ. Res.* **142**, 141–146. doi:10.1016/j.marenvres.2018.10.007
- Lüdecke, D., Ben-Shachar, M. S., Patil, I., Waggoner, P. and Makowski, D. (2021). performance: an R package for assessment, comparison and testing of statistical models. *J. Open Source Softw.* **6**, 3139. doi:10.21105/joss.03139
- MacKenzie, C. L., Ormondroyd, G. A., Curling, S. F., Ball, R. J., Whiteley, N. M. and Malham, S. K. (2014). Ocean warming, more than acidification, reduces shell strength in a commercial shellfish species during food limitation. *PLoS ONE* **9**, e86764. doi:10.1371/journal.pone.0086764
- Mahanes, S. A., Sorte, C. J. B. and Bracken, M. E. S. (2023). The functional effects of a dominant consumer are altered following the loss of a dominant producer. *Ecol. Evol.* **13**, e10342. doi:10.1002/ecs3.10342

- Marshall, K. E., Anderson, K. M., Brown, N. E., Dytterski, J. K., Flynn, K. L., Bernhardt, J. R., Konecny, C. A., Gurney-Smith, H. and Harley, C. D. (2021). Whole-organism responses to constant temperatures do not predict responses to variable temperatures in the ecosystem engineer *Mytilus trossulus*. *Proc. R. Soc. B* **288**, 20202968. doi:10.1098/rspb.2020.2968
- Masson-Delmotte, V., Zhai, P., Pirani, S., Connors, L., Péan, C., Berger, S., Caud, N., Chen, Y., Goldfarb, L., Gomis, M. I. et al. (2021). *Climate Change 2021: The Physical Science Basis. Contribution of Working Group I to the Sixth Assessment Report of the Intergovernmental Panel on Climate Change*. Cambridge University Press.
- Melzner, F., Stange, P., Trübenbach, K., Thomsen, J., Casties, I., Panknin, U., Gorb, S. N. and Gutowska, M. A. (2011). Food supply and seawater pCO₂ impact calcification and internal shell dissolution in the blue mussel *Mytilus edulis*. *PLoS ONE* **6**, e24223. doi:10.1371/journal.pone.0024223
- Miller, L. P. and Long, J. D. (2015). A tide prediction and tide height control system for laboratory mesocosms. *PeerJ* **3**, e1442.
- Mock, C. J. and Dodds, S. F. (2009). The Sitka Hurricane of October 1880. In *Historical Climate Variability and Impacts in North America* (ed. L.-A. Dupigny-Giroux and C. J. Mock), pp. 99–106. Springer.
- Mucci, A. (1983). The solubility of calcite and aragonite in seawater at various salinities, temperatures, and one atmosphere total pressure. *Am. J. Sci.* **283**, 780–799. doi:10.2475/ajs.283.7.780
- Pfister, C. A., Roy, K., Wootton, J. T., McCoy, S. J., Paine, R. T., Suchanek, T. H. and Sanford, E. (2016). Historical baselines and the future of shell calcification for a foundation species in a changing ocean. *Proc. R. Soc. B* **283**, 20160392. doi:10.1098/rspb.2016.0392
- Rangel, R. E. (2023). From individual to ecosystem: multi-stressor effects of acidification and warming on the physiological responses of coastal marine invertebrates. *PhD thesis*, University of California, Irvine.
- Rangel, R. E. and Sorte, C. J. B. (2022). Local-scale thermal history influences metabolic response of marine invertebrates to warming. *Mar. Biol.* **169**, 126. doi:10.1007/s00227-022-04110-2
- Rangel, R. E., Bracken, M. E. S., Kroeker, K. J., Miller, L. P. and Sorte, C. J. B. (2025). Data from: Factorial field manipulation reveals CO₂ and temperature effects on a critical habitat-forming shellfish. *Dryad*. doi:10.7280/D1P10V
- Ricart, A. M., Gaylord, B., Hill, T. M., Sigwart, J. D., Shukla, P., Ward, M., Ninokawa, A. and Sanford, E. (2021). Seagrass-driven changes in carbonate chemistry enhance oyster shell growth. *Oecologia* **196**, 565–576. doi:10.1007/s00442-021-04949-0
- Ries, J. B., Cohen, A. L. and McCorkle, D. C. (2009). Marine calcifiers exhibit mixed responses to CO₂-induced ocean acidification. *Geology* **37**, 1131–1134. doi:10.1130/G30210A.1
- Romanek, C. S., Grossman, E. L. and Morse, J. W. (1992). Carbon isotopic fractionation in synthetic aragonite and calcite: effects of temperature and precipitation rate. *Geochim. Cosmochim. Acta* **56**, 419–430. doi:10.1016/0016-7037(92)90142-6
- Rovero, F., Hughes, R. N. and Chelazzi, G. (1999). Cardiac and behavioural responses of mussels to risk of predation by dogwhelks. *Anim. Behav.* **58**, 707–714. doi:10.1006/anbe.1999.1176
- Ruela, R., Sousa, M., deCastro, M. and Dias, J. (2020). Global and regional evolution of sea surface temperature under climate change. *Glob. Planet. Change* **190**, 103190. doi:10.1016/j.gloplacha.2020.103190
- Rullens, V., Lohrer, A. M., Townsend, M. and Pilditch, C. A. (2019). Ecological mechanisms underpinning ecosystem service bundles in marine environments – a case study for shellfish. *Front. Mar. Sci.* **6**, 409. doi:10.3389/fmars.2019.00409
- Sanders, T., Schmittmann, L., Nascimento-Schulze, J. C. and Melzner, F. (2018). High calcification costs limit mussel growth at low salinity. *Front. Mar. Sci.* **5**, 352. doi:10.3389/fmars.2018.00352
- Seed, R. and Suchanek, T. H. (1992). Population and community ecology of *Mytilus*. In *The Mussel Mytilus: Ecology, Physiology, Genetics and Culture* (ed. E. Gosling), Vol. 25, pp. 87–170. Elsevier.
- Sherker, Z. T., Ellrich, J. A. and Scrosati, R. A. (2017). Predator-induced shell plasticity in mussels hinders predation by drilling snails. *Mar. Ecol. Prog. Ser.* **573**, 167–175. doi:10.3354/meps12194
- Silbiger, N. J. and Sorte, C. J. B. (2018). Biophysical feedbacks mediate carbonate chemistry in coastal ecosystems across spatiotemporal gradients. *Sci. Rep.* **8**, 1–11. doi:10.1038/s41598-017-18736-6
- Sorte, C. J. B. and Bracken, M. E. S. (2015). Warming and elevated CO₂ interact to drive rapid shifts in marine community production. *PLoS ONE* **10**, e0145191. doi:10.1371/journal.pone.0145191
- Sorte, C. J. B., Kroeker, K. J., Miller, L. P. and Bracken, M. E. S. (2023). Biological modification of coastal pH depends on community composition and time. *Ecology* **104**, e4113. doi:10.1002/ecy.4113
- Stillman, J. H., Amri, A. B., Holdreith, J. M., Hooper, A., Leon, R. V., Pruett, L. R. and Bukaty, B. M. (2025). Ecophysiological responses to heat waves in the marine intertidal zone. *J. Exp. Biol.* **228**, jeb246503. doi:10.1242/jeb.246503
- Suzuki, M. and Nagasawa, H. (2013). Mollusk shell structures and their formation mechanism. *Can. J. Zool.* **91**, 349–366. doi:10.1139/cjz-2012-0333
- Telesca, L., Peck, L. S., Sanders, T., Thyrring, J., Sejr, M. K. and Harper, E. M. (2019). Biomineralization plasticity and environmental heterogeneity predict geographical resilience patterns of foundation species to future change. *Glob. Change Biol.* **25**, 4179–4193. doi:10.1111/gcb.14758
- Telesca, L., Peck, L. S., Backeljau, T., Heinig, M. F. and Harper, E. M. (2021). A century of coping with environmental and ecological changes via compensatory biomineralization in mussels. *Glob. Change Biol.* **27**, 624–639. doi:10.1111/gcb.15417
- Tharaldson, T. M. (2018). The ability of *Phyllospadix* spp., a pair of intertidal foundation species, to maintain biodiversity and ameliorate CO₂ stress in rocky shore tidepools. MSc thesis, Cal Poly Humboldt.
- Thomsen, J., Gutowska, M., Saphörster, J., Heinemann, A., Trübenbach, K., Fietzke, J., Hiebenthal, C., Eisenhauer, A., Körtzinger, A., Wahl, M. et al. (2010). Calcifying invertebrates succeed in a naturally CO₂-rich coastal habitat but are threatened by high levels of future acidification. *Biogeosciences* **7**, 3879–3891. doi:10.5194/bg-7-3879-2010
- Thomsen, J., Casties, I., Pansch, C., Körtzinger, A. and Melzner, F. (2013). Food availability outweighs ocean acidification effects in juvenile *Mytilus edulis*: laboratory and field experiments. *Glob. Change Biol.* **19**, 1017–1027. doi:10.1111/gcb.12109
- Tunnicliffe, V., Davies, K. T., Butterfield, D. A., Embley, R. W., Rose, J. M. and Chadwick, W. W., Jr (2009). Survival of mussels in extremely acidic waters on a submarine volcano. *Nat. Geosci.* **2**, 344–348. doi:10.1038/ngeo500
- Vargas, C. A., Cuevas, L. A., Broitman, B. R., San Martín, V. A., Lagos, N. A., Gaitán-Espitia, J. D. and Dupont, S. (2022). Upper environmental pCO₂ drives sensitivity to ocean acidification in marine invertebrates. *Nat. Clim. Change* **12**, 200–207. doi:10.1038/s41558-021-01269-2
- Wahl, M., Schneider Covachá, S., Saderne, V., Hiebenthal, C., Müller, J., Pansch, C. and Sawall, Y. (2018). Macroalgae may mitigate ocean acidification effects on mussel calcification by increasing pH and its fluctuations. *Limnol. Oceanogr.* **63**, 3–21. doi:10.1002/lno.10608
- Wolfe, K., Nguyen, H. D., Davey, M. and Byrne, M. (2020). Characterizing biogeochemical fluctuations in a world of extremes: a synthesis for temperate intertidal habitats in the face of global change. *Glob. Change Biol.* **26**, 3858–3879. doi:10.1111/gcb.15103
- Yamada, S. B. and Boulding, E. G. (1998). Claw morphology, prey size selection and foraging efficiency in generalist and specialist shell-breaking crabs. *J. Exp. Mar. Biol. Ecol.* **220**, 191–211. doi:10.1016/S0022-0981(97)00122-6
- Zhao, X., Han, Y., Chen, B., Xia, B., Qu, K. and Liu, G. (2020). CO₂-driven ocean acidification weakens mussel shell defense capacity and induces global molecular compensatory responses. *Chemosphere* **243**, 125415. doi:10.1016/j.chemosphere.2019.125415